MCM-47: A Highly Crystalline Silicate Composed of Hydrogen-Bonded Ferrierite Layers

Allen Burton, Robyn J. Accardi, and Raul F. Lobo*

Center for Catalytic Science and Technology, Department of Chemical Engineering, University of Delaware, Newark, Delaware 19716,

Marco Falcioni and Michael W. Deem

Department of Chemical Engineering, University of California, Los Angeles, California 90095

Received March 20, 2000. Revised Manuscript Received June 27, 2000

The synthesis, structure solution, and characterization of the layered silicate MCM-47 are described. MCM-47 is synthesized using a diquaternary ammonium salt prepared from the reaction of 1-methylpyrrolidine with 1,4-dibromobutane. The structure solution of MCM-47 using Monte Carlo methods and the FOCUS algorithm shows that the material is composed of ferrierite layers. The Rietveld refinement of synchrotron X-ray powder diffraction data in space group *Cmcm* gives unit cell parameters $a = 7.386$ Å, $b = 22.454$ Å, and $c = 14.018$ Å and agreement values of $R_p = 5.20\%$, $R_{wp} = 6.99\%$, and $\chi^2 = 3.01$. The results of the structure refinement and the ^{1}H MAS NMR spectrum indicate that the layers of MCM-47 are held together by strong hydrogen bonds. Energy minimization calculations of the organic structure directing agent within the layers of MCM-47 suggest that geometric complementarity between the organic and inorganic components can explain the unusual stacking arrangement of the ferrierite sheets.

Introduction

The applications of zeolites in catalysis and adsorption are well-known,[1,2] yet these applications are limited to molecules smaller than the pore apertures of the zeolite. In this respect, layered materials are attractive as potential catalysts, adsorbents, and ion exchangers. Layered materials can be delaminated or pillared to produce high-surface-area materials with a majority of their active sites or cations exposed at the crystal surface.[3−5] MCM-22 is a recent example of a layered aluminosilicate that has attracted considerable interest as a solid acid,[3,4,6,7] and layered clays (such as montmorillonite) have been examined for a wide range of uses including selective adsorption of organic molecules, ion exchange, and gas separations.[5,8−12] Of particular interest are polymer/clay nanocomposite materials which have been investigated for use in ion conduction and reinforcement of polymer-based materials.[13−16]

To date, few detailed structures of synthetic layered silicates have been reported. This is in large part due either to poor crystallinity or to stacking disorder that often occurs between the noncovalently bound layers. The powder diffraction patterns of layered materials often suffer from severe peak broadening that precludes structure solution by ab initio methods. However, recently there has been an increased activity in the structure elucidation of layered silicates, including reports on kanemite,[17] PREFER,[18,19] RUB-15,[20] and RUB-18.[21,22] The powder XRD patterns of each of these materials indicate that they are highly crystalline with no stacking disorder among the layers. In each of these structures both electrostatic and hydrogen-bonding forces are vital in maintaining the highly ordered arrangements of silicate layers.

* Corresponding author.

(1) van Bekkum, H., Flanigen, E. M., Jansen, J. C., Eds.; *Introduction to Zeolite Science and Practice*; *Stud. Surf. Sci. Catal.* **1991**, *58*.
(2) Breck, D. W. *Zeolite Molecular Sieves*; John Wiley and Sons: New York, 1974.
(3) Corma, A.; Fornes, V.; Pergher, S. B. *Nature* **1998**, *396*, 353.
(4) Corma, A.; Fornes, V.; Martinez-Triguero, J.; Pergher, S. B. *J. Catal.* **1999**, *186*, 57.
(5) van Olphen, H. *An Introduction to Clay Colloid Chemistry*; John Wiley and Sons: New York, 1963.
(6) Corma, A.; Davis, M.; Fornes, V.; GonzalezAlfaro, V.; Lobo, R.; Orchilles, A. V. *J. Catal.* **1997**, *167*, 438.
(7) Corma, A.; Martinez-Triguero, J. *J. Catal.* **1997**, *165*, 102.
(8) McBride, M. B. *Environmental Chemistry of Soils*; Oxford University Press: New York, 1994.
(9) Theng, B. K. G. *The Chemistry of Clay Organic Reactions*; John Wiley and Sons: New York, 1974.
(10) Theng, B. K. G. *Formation and Properties of Clay-Polymer Complexes*; Elsevier: New York, 1979.
(11) Dyer, A.; Chow, J. K. K.; Umar, I. M. *J. Radioanal. Nucl. Chem.* **1999**, *242*, 313.
(12) Cool, P.; Clearfield, A.; Crooks, R. M.; Vansant, E. F. *Adv. Environ. Res.* **1999**, *3*, 151.
(13) Fischer, H. R.; Gielgens, L. H.; Koster, T. P. M. *Acta Polym.* **1999**, *50*, 122.
(14) Vaia, R. A.; Vasudevan, S.; Krawiec, W.; Scalon, L. G.; Giannelis, E. P. *Adv. Mater.* **1995**, *7*, 154.
(15) Giannelis, E. P. *Appl. Organomet. Chem.* **1998**, *12*, 675.
(16) Burnside, S. D.; Giannelis, E. P. *Chem. Mater.* **1995**, *7*, 1597.
(17) Vortmann, S.; Rius, J.; Marler, B.; Gies, H. *Eur. J. Mineral.* **1999**, *11*, 125.
(18) Schreyeck, L.; Caullet, P.; Mougenel, J. C.; Guth, J. L.; Marler, B. *Microporous Mater.* **1996**, *6*, 259.
(19) Schreyeck, L.; Caullet, P.; Mougenel, J. C.; Guth, J. L.; Marler, B. *Stud. Surf. Sci. Catal.* **1997**, *105*, 1949.
(20) Oberhagemann, U.; Bayat, P.; Marler, B.; Gies, H.; Rius, J. *Angew. Chem., Int. Ed. Engl.* **1996**, *35*, 2869.
(21) Vortmann, S.; Rius, J.; Siegmann, S.; Gies, H. *J. Phys. Chem. B* **1997**, *101*, 1292.
(22) Wolf, I.; Gies, H.; Fyfe, C. A. *J. Phys. Chem. B* **1999**, *103*, 5933.

10.1021/cm000243q CCC: $19.00
Published on Web 09/16/2000

Here we report the synthesis, structure solution, and characterization of MCM-47. The structure of MCM-47 was solved by Monte Carlo methods[23−25] and, independently, by the FOCUS method.[26] MCM-47 is a highly crystalline silicate composed of ferrierite layers. The distances between the silanol (≡Si−OH) and siloxy (≡Si−O$^-$) oxygen atoms in adjacent layers are the shortest reported for any zeolite or layered silicate. In addition to electrostatic and van der Waals interactions between the organic structure directing agent (SDA) and the silicate layers, hydrogen bonding plays a key role in maintaining the highly ordered stacking of ferrierite layers.

Experimental Section

Synthesis and Calcination. The organic structure directing agent (SDA) was prepared using the following procedure: 20.0 g (117 mmol) of 1-methylpyrrolidine (Aldrich) was dissolved in 100 mL of tetrahydrofuran. To this solution 12.7 g (58.7 mmol) of 1,4-dibromobutane (99% Aldrich) was added dropwise and allowed to react overnight with rapid stirring. The precipitated tetramethylene bis(*N*-methylpyrrolidinium) dibromide salt was quickly vacuum filtered and rinsed with acetone. The crude product was then recrystallized from 2-propanol by the addition of ethyl acetate and subsequently rinsed with ethyl ether. After purification, the hygroscopic SDA was stored in a desiccator to prevent adsorption of moisture.

MCM-47 was prepared according to the method of Valyocsik.[27] The gel composition used was 1 SiO_2:0.30 NaOH:40 H_2O: 0.12 tetramethylene bis(*N*-methylpyrrolidinium) dibromide. In a typical synthesis 0.25 g of NaOH (98% Aldrich) and 1.00 g of tetramethylene bis(*N*-methylpyrrolidinium) dibromide were dissolved in 12.07 g of H_2O. To this solution 4.19 g of 30% colloidal silica (Ludox 30) was added. The resulting gel was stirred for 15 min and then sealed in a 23 mL Teflon-lined Parr autoclave. The synthesis was carried out with continuous tumbling at 50 rpm for 5 days at 160 °C. After quenching the autoclaves in water, the white crystals were recovered by vacuum filtration, washed with 1 L of deionized water, and dried in an oven overnight at 100 °C.

Two calcination procedures were performed on MCM-47 which resulted in products with different "crystallinity". In the first procedure the temperature was maintained at 120 °C for 2 h, ramped at 2 °C/min to 550 °C, held at 550 °C for 12 h, and then allowed to cool to room temperature. For the second procedure, the temperature was maintained at 120 °C for 2 h, ramped to 250 °C at 0.5 °C/min, held at 250 °C for 12 h, ramped to 350 °C at 8.3 °C/h, held at 350 °C for 18 h, ramped to 540 °C at 10.5 °C/h, held at 540 °C for 12 h, and then finally allowed to cool to room temperature.

Analytical. Powder X-ray diffraction (XRD) patterns were obtained on a Phillips X'Pert diffractometer using Cu Kα radiation. The data were collected in step mode from 4 to 40° 2θ with a 0.02° step size. Synchrotron X-ray powder diffraction data were collected on the X3B1 beam line at Brookhaven National Laboratory. The as-made MCM-47 sample was packed into a 1 mm glass capillary, and the data were collected at ambient temperature using a step size of 0.005° from 2° to 44° 2θ with a wavelength of $\lambda = 0.6998$ Å. The peak deconvolution of the powder XRD was carried out using the Phillips package ProFit, and the unit cell was determined using the DICVOL91[28] program.

Nitrogen adsorption isotherms were collected at 77 K using a Micromeritics ASAP 2010 instrument. Micropore volume was determined at $P/P_0 = 0.1$ assuming a liquid nitrogen density of 0.81 g/cm^3. Thermogravimetric analysis (TGA) measurements were recorded with a Cahn TG-121 microbalance by heating the sample in air to 100 °C for 2 h, ramping the temperature at 2 °C/min to 700 °C, and holding the temperature at 700 °C for 6 h. Elemental analyses were performed by Galbraith Laboratories (Knoxville, TN). Scanning electron micrographs (SEM) were obtained out on a JEOL JXA-840 scanning microanalyzer with an accelerating voltage of 15 kV.

^{29}Si magic angle spinning (MAS) NMR experiments were performed using a 300 MHz Bruker MSL with a 7 mm probe. Samples were spun in zirconia rotors. The spectra were obtained by pulsing at a Larmor frequency of 59.627 MHz and spinning at a rate of 3 kHz. A $\pi/3$ pulse of 4 μs was implemented, and a recycle delay of 90 s was used between each scan. 3-(Trimethylsilyl)-1-propanesulfonic acid (DSS) was used as the chemical shift reference. ^{29}Si−{^{1}H} cross-polarization (CP) MAS spectra were obtained using high-power decoupling. A 4 μs $\pi/3$ pulse was used with a recycle delay of 90 s. Solid-state ^{1}H MAS NMR spectra were acquired on a Bruker Avance DSX 500 spectrometer operating at 500.13 MHz. The MAS spectra were obtained using a fast-spinning Bruker MAS probe with a 2.5 mm zirconia rotor. Spinning rates of 28 kHz were used to remove peak broadening due to homonuclear dipolar coupling. A standard $\pi/2$ pulse of 2.1 μs was used to record the spectra.

Two methodologies were used to determine the structure of MCM-47. In one approach, the structure of the as-made MCM-47 was determined by Monte Carlo methods.[23] In another approach, a topology produced using the FOCUS algorithm[26] was used to develop the structural model of MCM-47. A distance least-squares (DLS) refinement of the crystalline layered silicate structure determined from these methods was carried out with DLS-76.[29] The Rietveld refinement of the synchrotron powder XRD data was performed with GSAS.[30] Energy minimization calculations were performed using Cerius^2 2.1 from MSI with the Burchart-Universal force field.[31]

Results and Discussion

Preliminary Results. SEM micrographs (Figure 1) indicate that MCM-47 is composed of platelike crystallites that are approximately 1 μm in length and 0.1 μm in thickness. Figure 2a−c shows the powder XRD patterns of the as-made MCM-47 and the products that result from the two different calcination procedures. The peak positions in the XRD pattern of the as-synthesized sample are similar to those reported in the patent literature.[27] The powder XRD pattern is also very similar to the "unknown sample B" recently reported by Takewaki et al.,[32] who speculated that the structure is a ferrierite-like phase. However, there are some differences between the XRD patterns of these two materials, most notably two broad peaks before 6° 2θ (Cu Kα) that are present in the "unknown B" but absent in MCM-47.

The synchrotron powder XRD pattern (Figure 3) of the as-synthesized material was initially indexed in a monoclinic lattice with cell parameters $a = 7.393$ Å, $b = 11.823$ Å, $c = 14.030$ Å, and $\gamma = 108.2°$. This was later determined to be the primitive unit cell of a C-centered orthorhombic lattice with cell parameters $a = 7.393$ Å,

(23) Falcioni, M.; Deem, M. W. *J. Chem. Phys.* **1999**, *110*, 1754.
(24) Deem, M. W.; Newsam, J. M. *Nature* **1989**, *342*, 260.
(25) Deem, M. W.; Newsam, J. M. *J. Am. Chem. Soc.* **1992**, *114*, 7189.
(26) Grosse-Kunstleve, R. W.; McCusker, L. B.; Baerlocher, C. *J. Appl. Crystallogr.* **1997**, *30*, 985.
(27) Valyocsik, E. W. US Patent 5068096, 1991.
(28) Boultif, A.; Louer, D. *J. Appl. Crystallogr.* **1991**, *24*, 987.
(29) Baerlocher, C.; Hepp, A.; Meier, W. M. Distance Least Squares Refinement Program DLS-76, ETH, Zurich, 1977.
(30) Larson, A. C.; von Dreele, R. B. *General Structure Analysis System GSAS*; Los Alamos National Laboratory: Los Alamos, NM, 1994.
(31) Cerius^2 2.1 Product of MSI and Biosym.
(32) Takewaki, T.; Beck, L. W.; Davis, M. E. *Microporous Mesoporous Mater.* **1999**, *33*, 197.

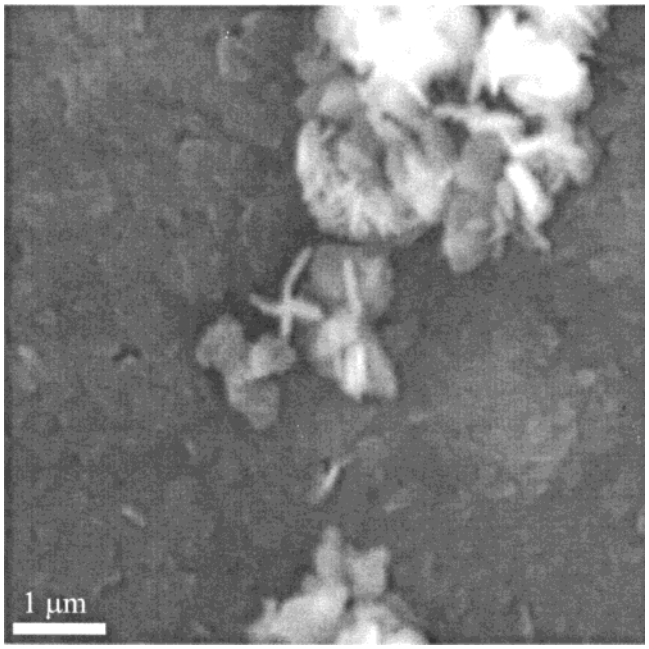

Figure 1. SEM micrograph of platelike crystallites of MCM-47.

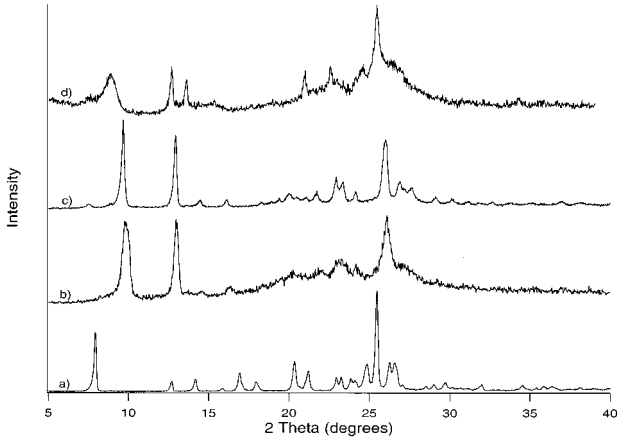

Figure 2. Powder X-ray diffraction (Cu Kα) of (a) as-synthesized MCM-47, (b) calcined MCM-47 (procedure A), (c) calcined MCM-47 (staged calcination, procedure B), and (d) as-synthesized MCM-47 treated with 0.1 M HCl. Note that the diffraction patterns for (b) and (c) were measured with identical scan parameters.

$b = 22.461$ Å, and $c = 14.030$ Å. The observed reflections are consistent with the space groups *Cmcm* (No. 63), *C*2*cm* (40), or *Cmc*2_1 (36). Examination of the synchrotron powder XRD pattern at low angles also reveals that the 111 reflection is much broader than the 020 and 002 reflections. This difference suggests that the smaller dimension of the thin crystallites corresponds to the *a*-direction. Simulations of the effects of the crystallite dimension on the powder XRD pattern (not shown) are also in qualitative agreement with this suggestion.

The *a* and *c* lattice parameters of MCM-47 are virtually identical to those observed within the layers of ferrierite (FER).[33] However, the *b* lattice parameter of MCM-47 is about 3.7 Å greater than the corresponding lattice parameter for ferrierite. A similar crystalline

(33) Treacy, M. M. J.; Higgins, J. B.; von Ballmoos, R. *Collection of Simulated XRD Powder Patterns for Zeolites*, 3rd ed.; Elsevier: New York, 1996.

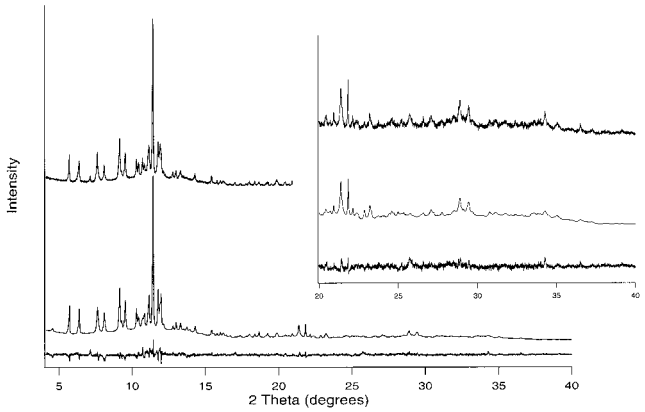

Figure 3. Experimental (top), simulated (middle), and difference profiles for the synchrotron powder X-ray diffraction pattern ($\lambda = 0.6698$ Å) of MCM-47. The 020 peak was excluded from the refinement (see text for details).

layered silicate composed of ferrierite layers (designated PREFER) has been reported,[18,19] but there are several differences between MCM-47 and PREFER. The first occurs in the spacing between the ferrierite layers; while MCM-47 has a *b* lattice dimension of about 22.5 Å, PREFER has a larger interlayer spacing indicated by a lattice dimension of 26.2 Å. A second difference is in the final products obtained after calcination of the as-made materials. PREFER can be heated to 550 °C to yield a thermally stable, highly crystalline ferrierite product formed from the condensation of the layers.[18,19] From Figure 2a−c it can be seen that there is a dramatic loss in crystallinity of the MCM-47 after calcination to 550 °C accompanied by the appearance of an amorphous background. This suggests that the silanol and siloxy groups between neighboring ferrierite layers are unable to fully condense in MCM-47, in contrast to what occurs during the calcination of PREFER. Comparison of parts b and c of Figure 2 also reveals that staged calcination yields a product with a better resolved XRD pattern. The difference in long-range order is further supported by the different nitrogen uptakes of the two materials (0.07 and 0.13 cm^3/g at $P/P_0 = 0.1$). It is also noteworthy that the *d* spacing of the 020 reflection changes from 11.23 Å in the as-made MCM-47 to about 9.15 Å in the calcined products. Although this gives a unit cell similar to that of ferrierite, the powder XRD pattern of the calcined material is very different. These data suggest that MCM-47 is composed of ferrierite layers that are stacked differently than the layers of PREFER.

Further evidence of the layered nature of MCM-47 is provided by the XRD pattern of MCM-47 that has been treated with an acid solution. Figure 2d shows the XRD pattern of an as-synthesized MCM-47 sample which has been treated with 0.1 M HCl at 100 °C for 1 day. While there is peak broadening and a decrease in *d* spacing for *hkl* reflections with nonzero *k* (most notably 020), the peak widths and positions of the *h*0*l* reflections remain unchanged after the acid treatments. These results are consistent with the presence of layers possessing two-dimensional order that remain intact after acid treatment.

Structure Solution by ZEFSAII. The framework structure of MCM-47 was determined using the Monte Carlo method ZEFSAII.[23] At this stage, only the monoclinic indexing was known, so space groups $P2_1/m$, $P2_1$, $P2$, Pm, and $P2/m$ were examined, and it was also

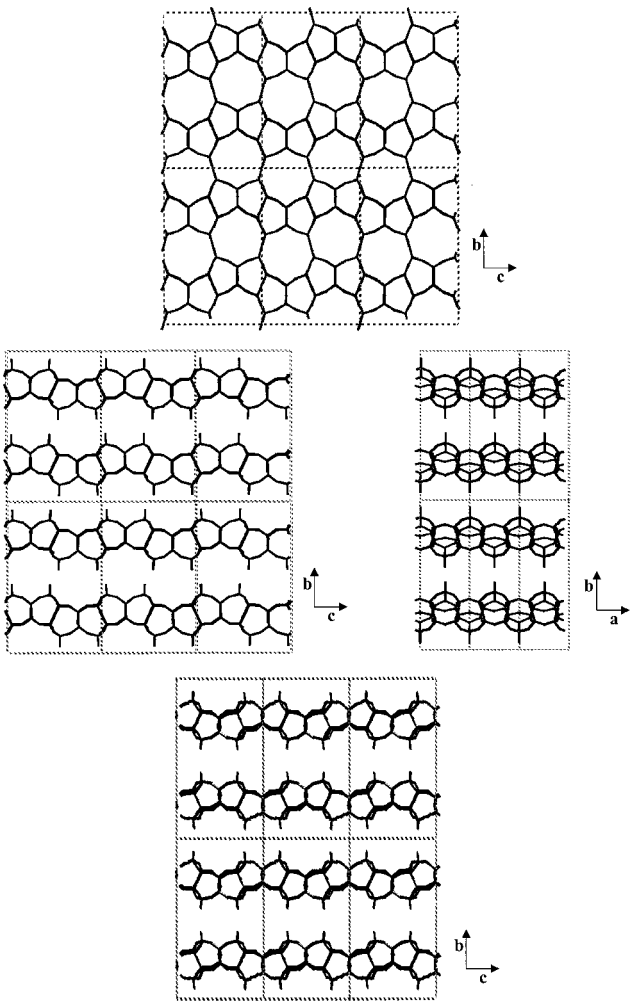

Figure 4. (a, top) Original framework topology obtained from ZEFSAII and FOCUS. (b, middle) Structure of MCM-47 (protons not shown for clarity) showing ferrierite layers in the $b-c$ plane and in the $a-b$ plane. (c, bottom) Structure of the layered silicate PREFER (reproduced from data provided in refs 18 and 19).

unknown that MCM-47 was a layered material. All densities in the range of 10−20 T atoms/1000 Å^3 were examined for each space group.

The presence of the disordered SDA and the low-symmetry monoclinic setting of the unit cell made it difficult to determine the structure without accounting for the scattering density of the SDA. We therefore incorporated one rigid SDA within the unit cell. The positional and rotational degrees of freedom of this molecule were optimized along with the positional degrees of freedom of the unique T atoms. The degrees of freedom of the SDA molecule entered the figure of merit in the Monte Carlo method only through the diffraction terms; energetic interactions between the SDA and framework atoms were not considered.

Of all the runs, only those in space group $P2_1/m$ gave possible structures. By far the best structure was found with six unique T atoms and 18 total T atoms in the unit cell (Figure 4a). This structure had the best match to the experimental diffraction pattern of all the possibilities considered. A parallel tempering run[23] confirmed this structure to be the best candidate. After it was determined that MCM-47 is a layered material, the long 3.9 Å Si−O−Si bonds between the layers could be severed and terminated with hydroxyls. The 3.9 Å bonds were formed because the parameters for ZEFSAII are optimized for 4-coordinate structures. The final structure has two pairs of T atoms that are topologically identical. This implies that there is a higher symmetry setting with only four unique T atoms. This higher symmetry setting is orthorhombic with space group *Cmcm*.

Structure Solution with FOCUS. The FOCUS algorithm[26] was also used to generate a series of possible frameworks. Although FOCUS is designed for the structure solution of fully connected tetrahedral frameworks, the results from FOCUS were used to infer the correct structure of MCM-47. The synchrotron powder XRD data ($\lambda = 0.6998$ Å) of the as-made MCM-47 were used as the input. All reflections between 3° and 37° 2θ were used for the Le Bail intensity extraction performed with GSAS.[30] Space groups *Cmcm*, *C*2*cm*, and *Cmc*2_1 were used in the topology searches. Frameworks with three rings were excluded from the topology search to limit consideration to viable structures. Only the high-symmetry space group *Cmcm* yielded a promising structure (Figure 4a). This structure possessed a highly strained framework composed of ferrierite layers. However, once the bonds between neighboring layers were broken, a DLS refinement yielded a structure with reasonable bond lengths and angles (Figure 4b).

Rietveld Refinement. The Rietveld refinement of the as-made MCM-47 from synchrotron X-ray diffraction data was performed using the space group *Cmcm*. The intense 020 peak was excluded from the refinement because of severe peak shape problems at low angles. Initial coordinates for the framework were taken from the DLS refinement of the layered structure topology. The framework and occluded organic structure directing agent of crystalline silicates or aluminosilicates often possess very different symmetries. However, since at ambient temperatures the organic species probably shows a high degree of dynamic and static disorder, the powder diffraction pattern of the "time- and space-averaged" structure can indicate an apparent symmetry that is equivalent to the symmetry of the framework. For these reasons we approximate the structure of the as-made MCM-47 with the *Cmcm* symmetry. Preliminary modeling of the powder XRD pattern of MCM-47 showed the best qualitative agreement with the experimental pattern when the organic was aligned along the *c*-direction. For the structure refinement, the SDA was modeled as a molecule of 1,1-dimethylcyclopentane to reduce the number of structural parameters from the organic component. However, this is still a good approximation of the diquaternary amine since the symmetry operations produce pyrrolidine rings separated by nearly the same distance expected within the SDA molecule.

The pseudo-Voigt function of Thompson et al.[34] and the asymmetry correction described by Finger et al.[35] were used to model the peak profiles. Constraints were placed on the silicon−oxygen bonds (1.60 ± 0.03 Å), the tetrahedral oxygen−oxygen distances (2.61 ± 0.05 Å), and the carbon−carbon bonds (1.54 ± 0.10 Å) through-

(34) Thompson, P.; Cox, D. E.; Hastings, J. B. *J. Appl. Crystallogr.* **1987**, *20*, 79.
(35) Finger, L. W.; Cox, D. E.; Jephcoat, A. P. *J. Appl. Crystallogr.* **1996**, *27*, 892.

Table 1. Structure Parameters of MCM-47 from Rietveld Refinement

atom	Wyckoff position	fractional occupancy	*x*	*y*	*z*	U_{iso} (×100 Å^2)
			Framework Atoms			
Si1	8g	1.0	0.2091(9)	0.2322(4)	1/4	0.49
Si2	16h	1.0	0.2971(7)	0.1881(3)	0.0460(4)	0.49
Si3	8f	1.0	0	0.1126(4)	0.5475(5)	0.49
Si4	4c	1.0	0	0.1739(4)	3/4	0.49
O1	16h	1.0	0.2548(12)	0.1920(4)	0.1604(4)	1.89
O2	4c	1.0	0	0.2466(7)	1/4	1.89
O3	8g	1.0	0.3189(5)	0.2910(4)	1/4	1.89
O4	16h	1.0	0.1822(8)	0.1368(4)	0.0001(7)	1.89
O5	8f	1.0	1/2	0.1688(5)	0.0267(8)	1.89
O6	8d	1.0	1/4	1/4	0	1.89
O7	8f	1.0	0	0.1324(4)	0.6579(3)	1.89
O8	8f	1.0	1/2	0.4606(4)	0.4514(10)	1.89
			Extraframework Atoms[a]			
C1	16h	0.25	0.7506	0.0352	0.2606	2.00
C2	16h	0.25	0.6278	−0.0221	0.2648	2.00
C3	16h	0.25	0.5629	−0.0892	0.2664	2.00
C4	16h	0.25	0.5241	−0.0234	0.2937	2.00
C5	16h	0.25	0.5742	0.0380	0.3060	2.00
C6	16h	0.25	0.5279	0.0164	0.4225	2.00
C7	16h	0.25	0.5264	−0.0084	0.4023	2.00

[a] These atoms are an approximation of the statically and dynamically disordered structure directing agent. See text for details.

out the refinement. Atoms of the same element type were constrained to have the same isotropic thermal displacement parameters.

In space group *Cmcm* the final agreement values for the refinement are R_p = 5.20% and R_{wp} = 6.99%. However, this (highest) topological symmetry possesses an oxygen located at an inversion center ($^1/_4$, $^1/_4$, 0) and yields physically unrealistic bond angles. A similar problem occurs in the refinement of ferrierite with space group *Immm*.[36] The refinements were therefore repeated in space groups *C*2*cm*, *Cmc*2$_1$, and *Pmnn*. Although these lower symmetry space groups approximately double the number of structural parameters to give a more poorly overdetermined set of data, they showed little or no improvement in the final agreement values. In addition, although hard constraints were used on the silicon and oxygen atoms, these space groups also gave Si2−O6−Si2 bridging angles which differ little from the 180° angle required by space group *Cmcm*. For these reasons we consider *Cmcm* to be the best approximation of the symmetry of MCM-47. Attempts to refine the O6 atom in positions split about the inversion center also did not improve the refinement or bond angle. Table 1 shows the final atomic parameters obtained from the Rietveld refinement. It should be noted that these values strongly reflect the constraints used throughout the refinement. However, the final results and agreement values are consistent with a chemically sensible structure, and the simulated XRD pattern closely matches the experimental data. The presence of the organic species within the structure coupled with the poor resolution of the powder pattern makes it difficult to pinpoint the true symmetry of the material.

Structure of MCM-47. Figure 4b shows a model of MCM-47 without the organic SDA. This structure is similar to PREFER (Figure 4c) except the alternating layers have been shifted half a unit cell in the *c*-direction. The layers in MCM-47 are related by half translations in both the *a*- and *b*-directions, whereas in FER (or PREFER) these layers are related by mirror planes. The spacing between layers in PREFER is also greater than in MCM-47. The greater hydrogen-bonding forces (in addition to the electrostatic and steric interactions between the SDA and the silicate layers) between the siloxy and silanol groups in MCM-47 keep the ferrierite layers more closely bound than the layers in PREFER.

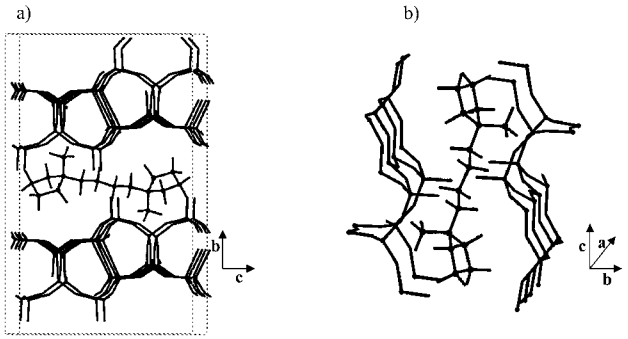

Figure 5. Projections showing lowest energy configuration of the tetramethylene bis(*N*-methylpyrrolidinium) molecule in MCM-47 in (a) the *b*−*c* plane and (b) the *b*−*c* plane (tilted) with only closest layer of atoms shown in order to highlight the channel pockets.

Energy minimization calculations were used to determine which configuration of the SDA optimizes the steric interactions within the layers of MCM-47. The electrically neutral analogues of the SDA and the silica framework were used in the calculations by replacing the organic nitrogens with carbon atoms and by terminating all siloxy groups with hydroxyls. In agreement with the Monte Carlo results and the refinement, the lowest energy is obtained with the organic aligned along the *c*-direction (Figure 5). It is interesting to note that the charge centers on the SDA are positioned near the charge centers of the silicate layers. In this configuration each of the pyrrolidine rings are also positioned beneath the pockets bound by the half six-ring units with the methyl groups pointing into these pockets (Figure 5b). In PREFER the spacing in the *c*-direction between the

(36) Weigel, S. J.; Gabriel, J.; Puebla, E. G.; Bravo, A. M.; Henson, N. J.; Bull, L. C.; Cheetham, A. K. *J. Am. Chem. Soc.* **1996**, *118*, 2427.

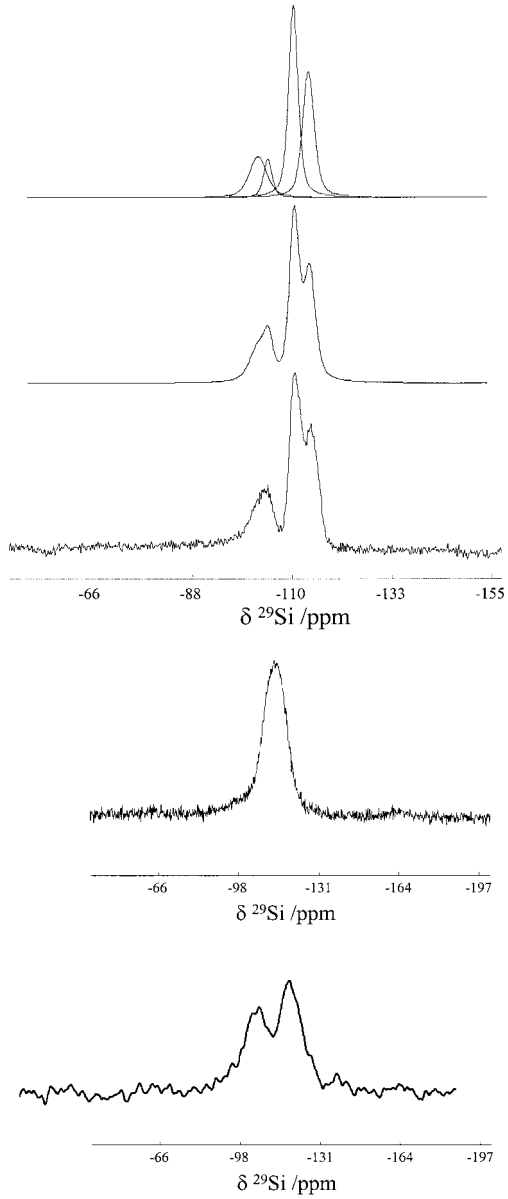

Figure 6. (a, top) Experimental pattern (bottom), simulated pattern (middle), and simulated components of the ^{29}Si MAS NMR spectrum of as-synthesized MCM-47. (b, middle) ^{29}Si MAS NMR spectrum of MCM-47 after staged calcination. (c, bottom) ^{29}Si−{^{1}H} CP MAS NMR spectrum of MCM-47 after staged calcination.

half six-ring units would not permit each methyl group to point within these pockets. This geometric complementarity may explain the unusual stacking of ferrierite layers in MCM-47.

Further evidence for the proposed model of MCM-47 is provided by the ^{29}Si MAS NMR spectrum shown in Figure 6a. Two Q^4 components (where Q^n stands for $X_{4-n}Si[OSi]_n$, X = OH or O^-) are observed at $\delta = -115.6$ and −112.0 ppm. The Q^3 signal was simulated with two components at $\delta = -105.7$ and −103.4 ppm. The heterogeneity of the Q^3 signal may be explained by examining Figures 5. Here it is seen that there are Q3 silicon atoms which differ in their spatial proximities to the pyrrolidine rings and the bridging tetramethylene group. The relative orientation of the pyrrolidine rings of the SDAs in neighboring layers also allows for the possibility of disorder in the as-made material; i.e., in some layers the rings will have the same position along the *b*-direction, while in others they may be related by translations of $\pm^1/_2$**b**.[37] Deconvolution of the spectrum indicates that approximately 33% of the Si atoms are given by the component at −115.6 ppm, 43% by the component at −112.0 ppm, and 24% by the Q^3 components. This agrees well with the population of Si atoms in different T sites expected from the proposed model: 33% for the sum of T1 (8) and T4 (4), 44% for T2 (16), and 22% for T3 (8).

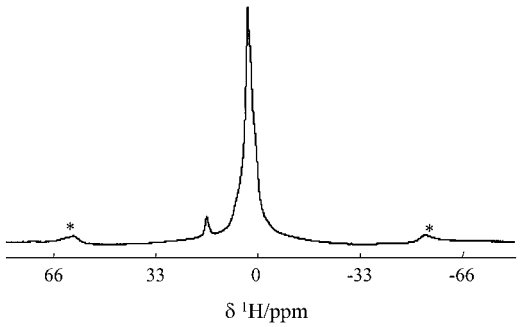

Figure 7. ^{1}H MAS NMR spectrum of MCM-47.

Figure 7 shows the ^{1}H MAS NMR spectrum of MCM-47. The intensities between 1.0 and 3.5 ppm are due to the resonances of the protons on the organic SDA, and the small shoulder near 6−7 ppm is probably due to water.[38] The sharp line at 16.6 ppm is due to silanol groups involved in strong hydrogen bonding with neighboring siloxy groups. This line represents about 4% of the total integrated intensity, which is within experimental error of the intensity expected from the model of MCM-47. Correlations developed by Eckert et al.[39] indicate that this ^{1}H chemical shift corresponds to an O···O distance of 2.4 Å, in close agreement with the distance obtained from the crystallographic model.[40] To our knowledge, this is the largest ^{1}H chemical shift reported for a silanol in any zeolite or layered silicate. In the spectra of as-made high silica zeolites synthesized with quaternary ammonium SDA's, the silanol resonance associated with the defects usually occurs around 10.2 ppm,[38] indicating an O···O distance of about 2.7 Å. A ^{1}H chemical shift of 15.9 ppm for RUB-18 is the closest reported for any other layered silicate.[22]

The results of the chemical analysis and TGA measurement of MCM-47 are also in excellent agreement with the proposed model. Chemical analysis indicates a Si/C ratio of 1.27, a C/N ratio of 7.03, and a Na/Si ratio less than 0.006. This is very close to the ideal formula (on a half unit cell basis) $Si_{18}O_{36}(OH)_2 \cdot C_{14}N_2H_{30} \cdot 2H_2O$. In the TGA experiment there is a 2.8% mass loss event between room temperature and 200 °C and then a 19.1% mass loss event which begins at 250 °C. Charge

(37) We considered the possibility that the broad 111 peak might be due to disorder of the SDA in the **a**-direction. We simulated the diffraction patterns of the faulted polymorphs using DiFFaX. The end polymorphs (and therefore the faulted polymorphs) were virtually indistinguishable from each other, and no differences among the polymorphs could be observed in the shape of the 111 peak. Thus, even though the SDA is probably disordered, it has very little effect on the X-ray diffraction pattern.

(38) Koller, H.; Lobo, R. F.; Burkett, S. L.; Davis, M. E. *J. Phys. Chem.* **1995**, *99*, 12588.

(39) Eckert, H.; Yesinowski, J. P.; Silver, L. A.; Stolper, E. M. *J. Phys. Chem.* **1988**, *92*, 2055.

(40) The distance from the refinement is sensitive to the Si−O bond length constraints used; both the original DLS model and the refinement without constraints yield a distance of 2.4 Å, whereas the refinement with constraints yields a distance of 2.2 Å.

balance dictates the presence of two silanol/siloxy pairs for each SDA molecule. For calcination to high temperatures, the oxidation of each SDA molecule should also result in the elimination of two OH groups from the silicate structure. If the initial mass loss is assigned to water, then the initial mass loss corresponds to about 2 H_2O/SDA (1 H_2O/charge). The second mass loss event corresponds to 1 SDA/17.7 Si atoms, which is very close to 1 SDA/18 Si atoms expected from the ideal model.

Structure of Calcined MCM-47. After the staged calcination to 540 °C, we expect approximately half of the silanol and siloxy groups to condense and thereby fuse the ferrierite layers. Although this implies that about 11% of the silicon atoms remain in a Q^3 coordination environment, it is difficult to distinguish the Q^4 and Q^3 components in the ^{29}Si NMR spectrum of the material obtained after the staged calcination (Figure 6b). The broad peak of this spectrum is evidence for a material with a large variation in $SiO_{4/2}$ coordination environments; i.e., a not well-ordered structure. Nonetheless, the $^{29}Si-\{^1H\}$ CP MAS NMR spectrum (Figure 6c) does support the presence of a large proportion of remaining silanols.

Since the powder X-ray diffraction pattern of calcined MCM-47 is different from that of ferrierite, the layers of MCM-47 do not fully condense as they do in PREFER. Figure 4c shows that in PREFER every silanol is opposed by a siloxy or silanol in the next layer. Upon calcination every silanol/siloxy pair can condense to yield a fully connected framework. However, in MCM-47 the silanol/siloxy groups in one layer do not directly oppose the siloxy/silanol groups in the next layer; the layers must shift in the *c*-direction to allow condensation of the siloxy/silanol pairs. If one layer shifts relative to another by half a unit cell in the *c*-direction, then full condensation (as in PREFER) of the layers in MCM-47 would be possible. It is more likely that the layers only shift by about 1/10 *c* so that the nearest siloxy/silanol pairs condense, but this implies that half of the pairs remain uncondensed since this slight shift also moves half of the silanols farther from their siloxy counterparts in the neighboring layer.

Since presumably each of the ferrierite layers in MCM-47 can shift in either the positive or negative *c*-direction, there is the possibility of disorder in the final calcined structure. The "pure" polymorphs of such a structure would be represented by either an ABAB or an ABCDE... arrangement of layers. DiFFaX[41,42] simulations of the powder X-ray diffraction patterns for the possible disordered structures are shown in Figure 8. Surprisingly, the simulated powder XRD for the pure ABAB polymorph most closely matches that of the experimental pattern. Although attempts were made to find an appropriate unit cell for the calcined material, the lack of well-resolved peaks prevented a reliable indexing. However, there are several peaks in the experimental pattern not predicted by the ABAB model which suggest a lowering of symmetry. There may even be slight shifts (or disorder) in the *a*-direction as well as a slight probability of forming FER-like domains. Further details of the structure of the calcined material are beyond the scope of this report and require more investigation.

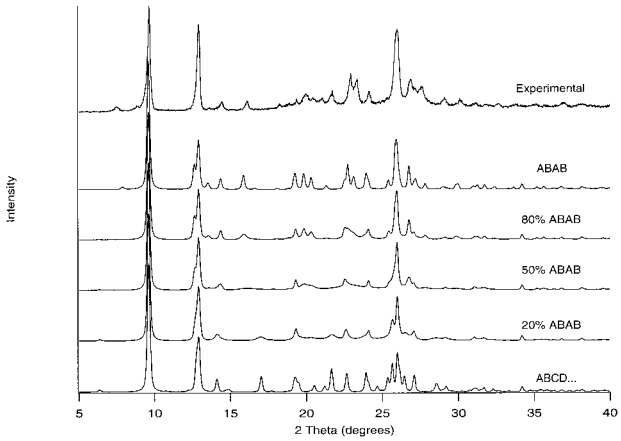

Figure 8. DiFFaX simulations of possible disordered polymorphs obtained after staged calcination of MCM-47.

Conclusions

The synthesis and characterization of the novel layered silicate MCM-47 have been reported. The structure of MCM-47 has been solved using the ZEFSAII Monte Carlo method and the FOCUS algorithm. MCM-47 is composed of ferrierite layers which are stacked differently than in PREFER, a layered precursor of ferrierite. The layers of MCM-47 are held together by electrostatic interactions between the diquaternary ammonium structure directing agent and the siloxy ($\equiv Si-O^-$) groups in the ferrierite layers. The hydrogen bonds between the siloxy groups and silanol groups in adjacent layers are also the strongest observed in any recently reported layered silicate. Unlike the zeolitic precursors PREFER and ERB-1,[43] the layers of MCM-47 do not fully condense upon calcination to form a completely connected framework.

Acknowledgment. R.F.L. and A.B. thank R. Grosse-Kunstleve for help with the use of the FOCUS algorithm, Z. Wang for assistance in collection of the SEM photographs, and D. Shantz for useful discussions. We are indebted to P. Stephens and S. Pagola for collection of the synchrotron data and to H. Koller and M. Kalwei for help with the collection of the ^1H MAS NMR spectra. R.F.L. acknowledges the financial support of Praxair, the DRP program of the state of Delaware, and the National Science Foundation through an international award. M.W.D. is grateful for support of Molecular Simulations Inc., Chevron Research and Technology Co., the Petroleum Research Fund through Grant 33312-G5, and the National Science Foundation through Grant CTS-9702403. This research was carried out in part at the National Synchrotron Light Source at Brookhaven National Laboratory, which is supported by the US Department of Energy, Division of Materials Sciences and Division of Chemical Sciences. The SUNY X3 beamline at NSLS is supported by the Division of Basic Energy Sources of the US Department of Energy under Grant DE-FG02-86ER45231.

CM000243Q

(41) Treacy, M. M. J.; Newsam, J. M.; Deem, M. W. *Proc. R. Soc. London A* **1991**, *443*, 449.

(42) Treacy, M. M. J.; Vaughan, D. E. W.; Strohmaier, K. G.; Newsam, J. M. *Proc. R. Soc. London A* **1996**, *452*, 813.

(43) Millini, R.; Perego, G.; Parker, Jr., W. O.; Bellussi, G.; Carluccio, L. *Microporous Mater.* **1995**, *4*, 221.